

BARE ICE FIELDS DEVELOPED IN THE INLAND PART OF ANTARCTICA

Shuhei TAKAHASHI¹, Tatsuo ENDOH², Nobuhiko AZUMA^{3*},
and Shigemi MESHIDA⁴

¹*Kitami Institute of Technology, Koen-cho 165, Kitami 090*

²*Institute of Low Temperature Science, Hokkaido University, Kita-19,
Nishi-8, Kita-ku, Sapporo 060*

³*Faculty of Technology, Hokkaido University, Kita-13, Nishi-8,
Kita-ku, Sapporo 060*

⁴*Japan Meteorological Agency, 3-4, Otemachi 1-chome,
Chiyoda-ku, Tokyo 100*

Abstract: Observations of a bare ice field was carried out at Seal Rock in the Sør Rondane area, East Antarctica. A large sublimation rate, 200 to 280 mm/a, was observed on the bare ice field. Air temperature on the bare ice was about 1°C higher than that on snow surface. The large sublimation rate was explained from the low albedo of bare ice; its value was roughly estimated from heat budget considerations. The bare ice fields were classified into 4 types according to origin.

1. Introduction

Bare ice fields are found locally in the inland region of Antarctica. On the surface of the bare ice fields, meteorites are often found. For the mechanism of the concentration of meteorites on the bare ice surface, NAGATA (1978) suggested that the ice flow transports meteorites to the surface. The large ablation from the bare ice surface should compensate in order to maintain the steady surface topography. However, the reason for the large ablation was not sufficiently studied in the previous studies.

From 1989 to 1990, the ablation on a bare ice field was observed in the Sør Rondane area, East Antarctica. In this report, the mechanisms of development of a bare ice field are discussed on the basis of the observation, and a classification of bare ice fields is suggested.

2. Observation at a Bare Ice Field at Seal Rock

Ablation and meteorological observations were carried out on a bare ice field leeward of Seal Rock (71°31'S, 24°05'E, 950 m a. s. l.) in the Sør Rondane Mountains area, East Antarctica, between January 1989 and January 1990. The topography of the bare ice field is shown in Fig. 1, in which contour lines are obtained from a rough survey; the distance was measured by the range meter of a snow vehicle and the relative height is estimated with eye.

* Present address: Nagaoka Technology and Science Institute, Kamitomioka 1630-1, Nagaoka 940-21.

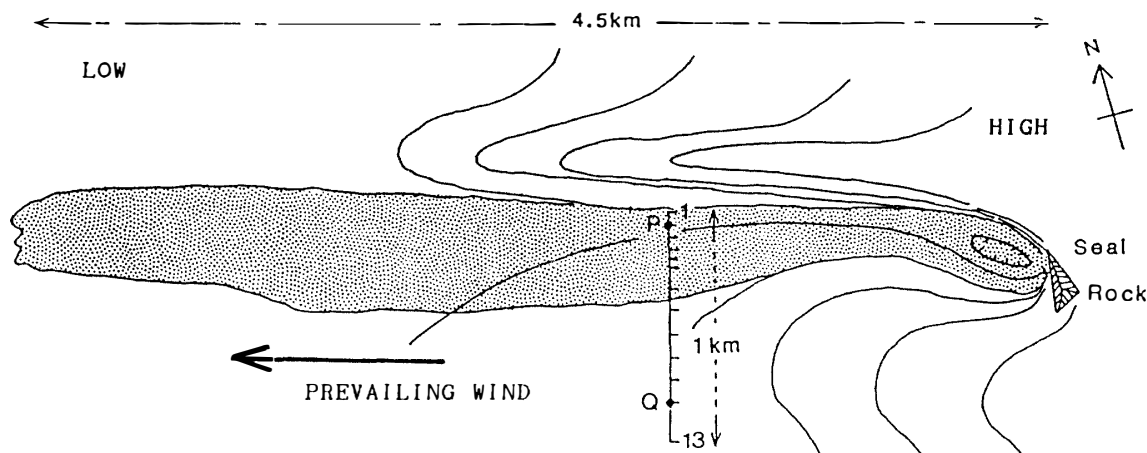


Fig. 1. Observation points at Seal Rock in Sør Rondane area, East Antarctica. P and Q: meteorological observation points on bare ice surface and snow surface respectively. Numbers show snow stake position for ablation observation. Contour lines roughly represent topography and each interval is 10 m.

Air temperature and wind speed were observed at two points, P and Q, as shown in Fig. 1. P is on a bare ice surface, and Q is on a deposited snow surface around the bare ice field (Fig. 2a, b and c). Air temperature was measured by thermistor sensors and wind speeds by 3-cup anemometers at 1.8 m height; the data were recorded by digital data loggers. All data were normally recorded between January 5 and 29 in 1989. However, in the following period (between February 1989 and January 1990), only one data logger of the temperature at Q was worked; other loggers were stopped by battery trouble.

Surface net mass balance was observed by the snow stake method. Snow stakes were set along a 1-km line with distances of 50–200 m transverse to the ice field, as shown in Fig. 1. By measuring the height of snow stakes, the changes of snow surface levels were measured 6 times from January 1989 to January 1990.

3. Results of Observations

3.1. Surface mass balance observation

The observed surface level change and surface mass balance at every snow stake are shown in Table 1. The surface mass balance was obtained from the level change and the densities of ice (0.92 g/cm^3) and snow (0.40 g/cm^3). Stakes No. 1–5 are on a bare ice surface, No. 6–8 are on mixed ice and snow surfaces, and No. 9–13 are on the deposited snow surface around the bare ice field. As shown in Fig. 3, large sublimation from the surface, 200 to 280 mm/a (water equivalent), was observed on the bare ice surface, and large accumulation of about 150 mm/a on the deposited snow surface.

3.2. Meteorological observation

The daily maximum and minimum temperature on the deposited snow surface (at Q) from January 1989 to January 1990 are shown in Fig. 4. The maximum temperature was about -7°C in January and the minimum temperature was about -42°C

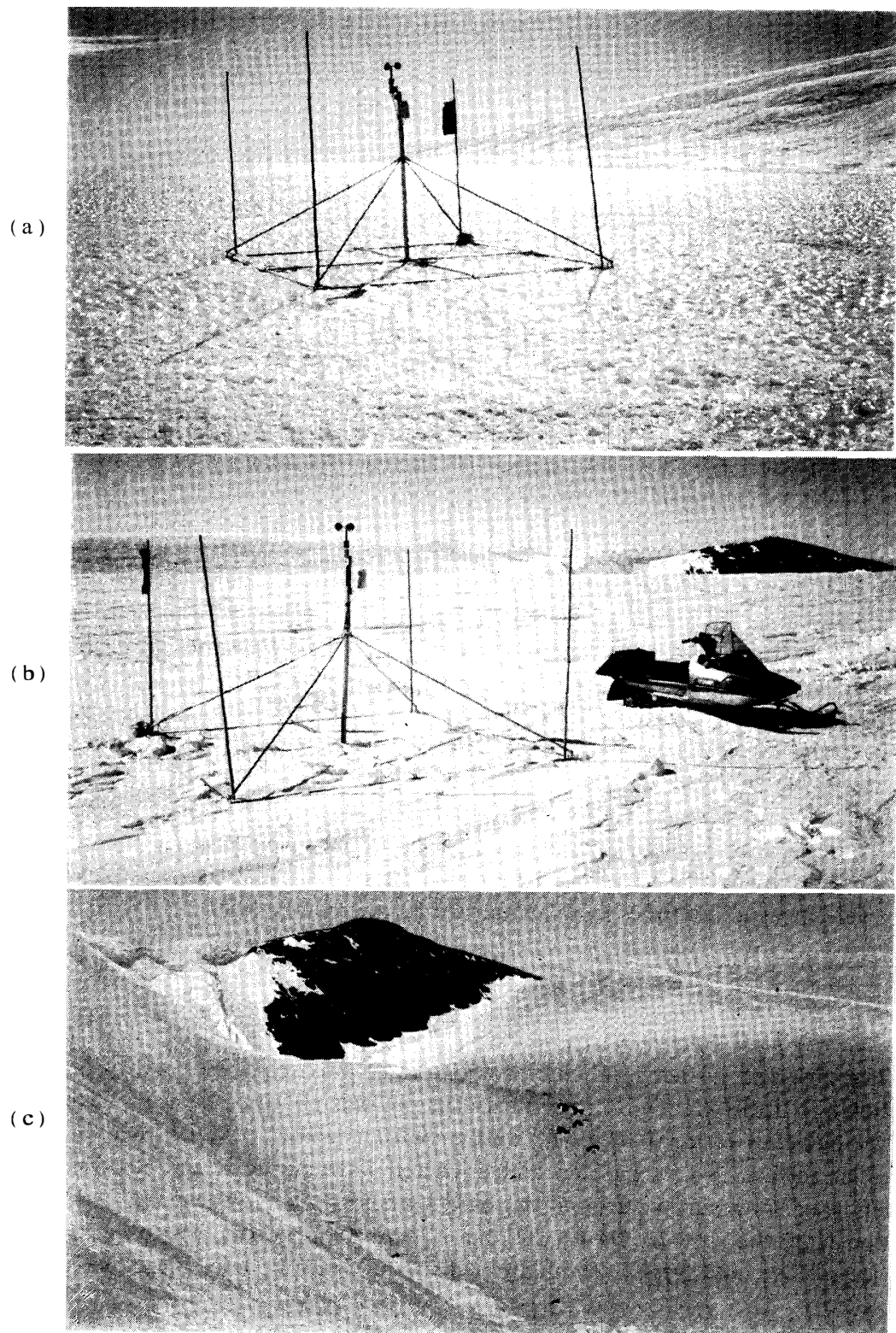


Fig. 2. Scenery of bare ice fields at Seal Rock. (a), (b): Meteorological observation points on bare ice surface and snow surface respectively. (c): Seal Rock from the leeward.

Table 1. Surface level change and surface net mass balance on a bare ice field at Seal Rock from January 1989 to January 1990.

No.	X (m)	C	Surface level change (cm)					Total 388d	Net balance (mm/a)
			Jan. 7 32d	Feb. 8 79d	Apr. 28 123d	Aug. 29 104d	Dec. 11 50d		
1	0	i	-6	-4	-7	-10	-6	-33	-285
2	50	i	-4	-2	-9	-7	-4	-26	-224
3	100	i	-4	-4	-6	-8	-3	-25	-216
4	150	i	-3.5	1	-8	-7	-6	-24	-207
5	200	i/s	-2	-2	-5	0	-6	-15	-129
6	250	i/s	-2	-1	-4	9	-10	-8	-64
7	350	i/s	-8	6	9	3	-9	1	4
8	450	s	-3	3	8	-4	-4	0	0
9	550	s	3.5	20	-13	8	-5	13	49
10	600	s	26	-11	-6	25	7	41	154
11	750	s	32	10	-8	13	-5	42	158
12	850	s	44	5	-12	4	1	42	158
13	1050	s	11	-10	-6	16	4	15	56

X: distance from No. 1 stake. C: surface condition (i: ice, s: snow, i/s: ice and snow partly exist). Net balance was obtained from the level change and the density of ice (920 kg/m^3) and snow (400 kg/m^3).

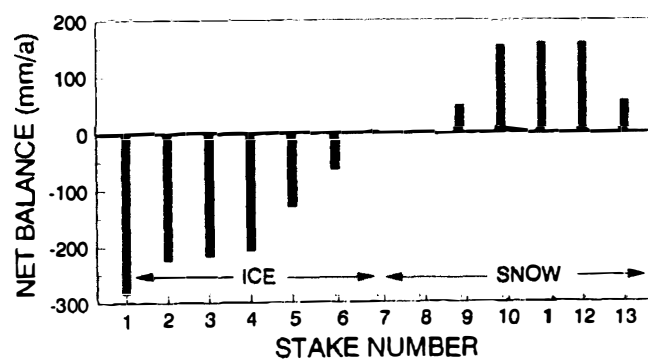


Fig. 3. Surface net balance obtained by the snow stake method. Observation points of each stake are shown in Fig. 1.

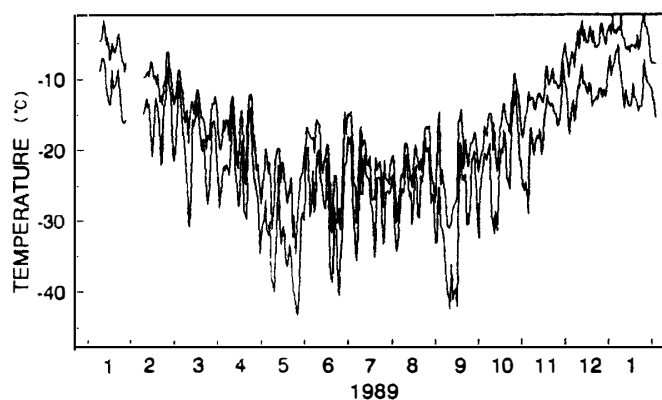


Fig. 4. Annual variation of the daily maximum and minimum air-temperature at Q (on a snow surface).

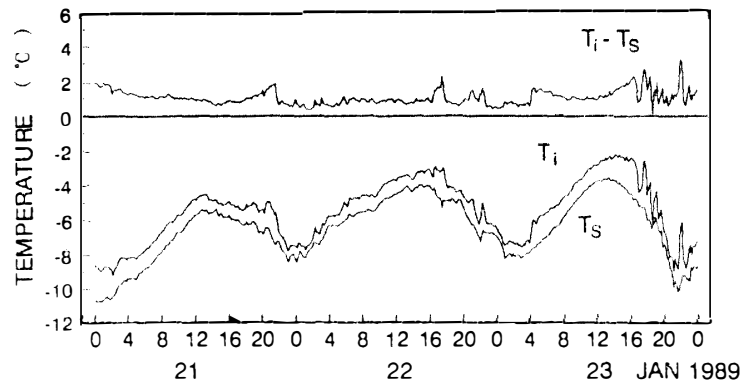


Fig. 5. Air temperature on the bare ice surface and the snow surface (January 21–23, 1989). T_i : temperature on bare ice, T_s : temperature on snow, and DT : $T_i - T_s$.

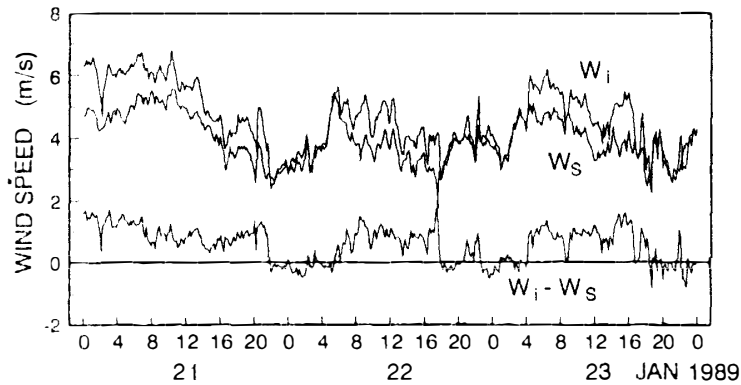


Fig. 6. Wind speed on the bare ice surface and the snow surface (January 21–23, 1989). W_i : wind speed on bare ice, W_s : wind speed on snow, and DW : $W_i - W_s$.

in May and September. The temperature variation was “pan-bottom type”; the temperature in winter was low and steady over a long period.

In Fig. 5, the air temperatures at P and Q and their difference are shown. On the average, the temperature on bare ice surface (at P) was about 1 to 2°C higher than the temperature on snow surface. The difference reflects the higher surface temperature on bare ice than on snow, which would be caused by the difference of net short-wave radiation owing to the albedo difference.

In Fig. 6, wind speeds at P and Q are shown. The mean wind speed on the ice surface is slightly larger than on the snow surface, about 0.5 m/s, which reflects the small roughness height on the bare ice surface. Adding to it, the variation of wind speed over the ice surface was larger than that over the snow surface. This suggests the existence of the turbulence due to Seal Rock, which causes increased sensible and latent heat fluxes.

4. Mechanism of Development of Bare Ice Field

4.1. Heat budget on bare ice fields

The sublimation from a bare ice surface was very large in summer. This large sublimation is caused by its low albedo. Once a bare ice surface is formed for some

reason, the albedo becomes lower, more solar radiation is absorbed, and sublimation from the surface is enhanced.

The seasonal variation of sublimation at Mizuho Station, Antarctica, in 1982 is shown in Fig. 7, which was observed by weighing a sublimation pan filled with ice every day. In the winter season of no solar radiation, condensation on the surface was observed, although the amount was small. In spring, the sublimation rapidly increased with increasing solar radiation, and became large in summer. Annual sublimation in 1982 was about 50 mm; almost the same result in 1977 was reported by FUJII and KUSUNOKI (1982).

The sublimation from the surface at Mizuho Station was well correlated with the solar radiation as shown in Fig. 8, in which the positive values of sublimation (evaporation) in Table 2 are plotted. In the Table 2, the sublimation is the monthly value of 1982, but the solar radiation is the monthly value of 1980 (KOKURITSU KYOKUCHI KENKYŪJO, 1985), because the continuous observation of solar radiation is only in 1980. The occasional observation of monthly solar radiation in other years showed similar values to the data of 1979. Therefore, the monthly value of 1980 would be representative in this area.

The recursive relation between the sublimation E (mm/d) and the solar radiation I (W/m^2) is

$$E = aI^b, \quad (1)$$

where

$$a = 4.20 \times 10^{-8}$$

$$b = 2.73.$$

The power b is about 3. The reason for this large power and the physical meaning of this power relation is a future subject.

The sublimation should be concerned with the net short-wave radiation $Q_{RS} = (1-A)I$, where A is albedo. Therefore, the ratio of sublimation between the two surfaces of different albedo is

$$E_2/E_1 = ((1-A_2)/(1-A_1))^b, \quad (2)$$

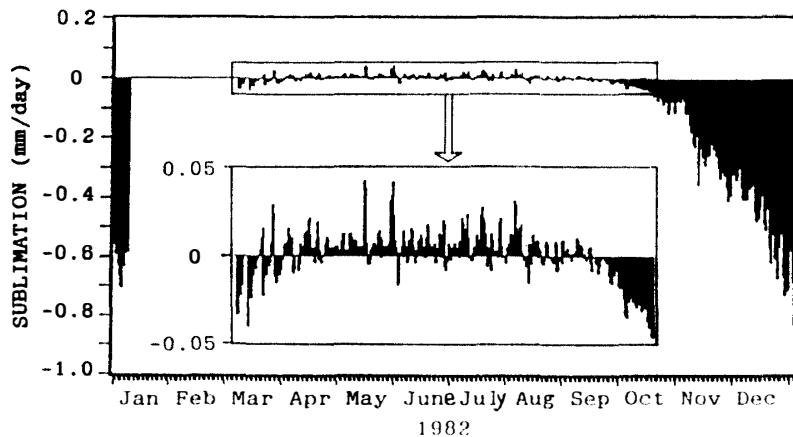


Fig. 7. Sublimation at Mizuho Station, Antarctica, from March 1982 to January 1983 observed using a sublimation-pan.

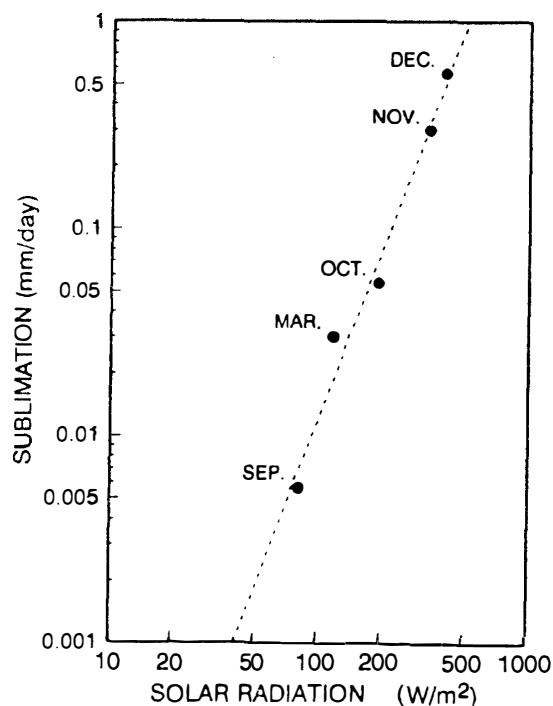


Fig. 8. Relation between sublimation and global solar radiation at Mizuho Station.

Table 2. Sublimation and solar radiation at Mizuho Station (positive value means evaporation).

	Sublimation (mm/day)	Solar radiation (W/m ²)
January		338
February		232
March	0.0300	118
April	-0.0055	31
May	-0.0093	1.5
June	-0.0040	0.0
July	-0.0080	0.5
August	-0.0034	16
September	0.0056	82
October	0.0545	192
November	0.2984	330
December	0.5630	397

where E_1 and E_2 are the sublimation on surfaces of albedo A_1 and A_2 . Adopting the snow surface albedo of 0.8 (YAMANOUCHI, 1983) and the bare-ice surface albedo of 0.5 (GRENFELL and PEROVICH, 1984) as A_1 and A_2 respectively, the ratio E_2/E_1 is 12.2. Therefore, from the annual sublimation of 50 mm/a at Mizuho Station, the annual sublimation on a bare ice surface is roughly estimated as 670 mm/a, though this estimated value is too large compared with the observed value (about 200 to 300 mm/a). The reason of overestimation can be in the eq. (1), which is the relation only for a snow surface. To estimate the sublimation on a bare-ice surface, the difference of thermal properties between snow and ice should be taken into account, as follows.

Considering that the net radiation Q_{NR} is a heat source on a surface and the

other heat fluxes are heat sinks, the heat balance on the surface can be expressed as

$$Q_{NR} = Q_S + Q_L + Q_C, \quad (3)$$

where Q_S sensible heat flux, Q_L latent heat flux, Q_C heat conduction to sub-surface layer. Q_{NR} is described as

$$Q_{NR} = (1-A)I + Q_{RL\downarrow} - \sigma T_s^4, \quad (4)$$

where A is albedo, I is global solar radiation, $Q_{RL\downarrow}$ is the downward long-wave radiation (celestial long-wave radiation), σ is the Stefan-Boltzmann constant and T_s is the surface temperature. OHATA *et al.* (1985) obtained the each components at Mizuho Station in the summer season (December in 1980); $Q_{NR} = 19.9 \text{ W/m}^2$, $Q_S = 7.4 \text{ W/m}^2$, $Q_L = 7.8 \text{ W/m}^2$ and $Q_C = 6.35 \text{ W/m}^2$.

If the solar radiation increases, the surface temperature also increases and therefore the sublimation rapidly increases with increase of the vapor pressure on the surface. The eq. (1), the relation between sublimation and solar radiation on a snow surface, is explained as a result of this change of sublimation due to the surface-temperature change.

The low albedo of a bare ice surface would produce the same result as the increase of solar radiation in eq. (4). However, the different thermal properties of ice would produce a different surface temperature.

If the snow or ice body is heated by a conductive heat flux Q_C from the initial condition of equi-temperature, the change of surface temperature dT after t sec is

$$dT = 2Q_C(t/\pi\rho C\lambda)^{1/2}, \quad (5)$$

where ρ is density of snow or ice, C is specific heat and λ is heat conductivity. As $\rho = 420, 920 \text{ kg m}^{-3}$, $C = 2.09, 2.10 \times 10^3 \text{ Jkg}^{-1} \text{ K}^{-1}$, $\lambda = 0.42, 2.24 \text{ Wm}^{-1} \text{ K}^{-1}$ for snow and ice respectively, the ratio of dT for an ice surface to that for a snow surface dT_{ice}/dT_{snow} is 0.292. This means that conductive heat easily flows in an ice body to under-surface rather than in snow.

The latent heat flux Q_L can be written by a bulk formula:

$$Q_L = \beta V(E_s - E), \quad (6)$$

where β is a bulk coefficient, V is wind speed, and E_s and E are the vapor pressure on a surface and in air respectively. If only the surface temperature changes, the change of Q_L can be written as

$$dQ_L = \beta V dE_s. \quad (7)$$

A convenient approximation for the saturation vapor pressure E_s over an flat ice-surface is (DE QUERVAIN, 1973)

$$E_s = E_0 \exp [k(T_s - T_0)], \quad (8)$$

where E_0 is the vapor pressure on the surface temperature of T_0 and k is a constant of $0.0857 \text{ (K}^{-1}\text{)}$. For the two surface-temperature changes dT_1 and dT_2 , the ratio of

the changes of latent heat flux, dQ_{L2}/dQ_{L1} , is written from eqs. (7) and (8) as

$$\begin{aligned} dQ_{L2}/dQ_{L1} &= dE_{S2}/dE_{S1} \\ &= dT_{S2}/dT_{S1}(1+k(dT_{S2}-dT_{S1})/2) . \end{aligned} \quad (9)$$

From dT_{ice}/dT_{snow} of 0.292, the ratio dQ_{L2}/dQ_{L1} for ice and snow are given by the eq. (9). If $dT_{ice}-dT_{snow}$ is supposed to be -5°C , dQ_{L2}/dQ_{L1} is 0.029 ($=0.785 dT_{S2}/dT_{S1}$). By multiplying this ratio to the former estimated sublimation 670 mm/a, which was calculated only from albedo difference on a snow surface, the sublimation on a bare-ice surface is estimated as 153 mm/a.

Owing to the difference of thermal properties of snow and ice, the surface temperature on ice can be considered to be lower than on snow as described above. With this surface temperature lowering, Q_s , Q_L and $(Q_{RL}\downarrow - \sigma T_s^4)$ decrease, and Q_C contrarily increases to compensate for the deficit, while $(1-A)I$ is constant. Therefore, according to eq. (5), the difference of surface temperature between ice and snow would not be so large, and the evaluated dT_{ice}/dT_{snow} , 0.292, should be corrected to be larger. Thus, the latter estimation of sublimation 153 mm/a is the minimum estimation, and 670 mm/a is the maximum value. More precise estimation requires the surface-temperature observation on the field, which is a problem for the future.

4.2. Redistribution of accumulation by drifting snow

Though the development of bare ice field is related to sublimation as explained above, the next question is how the bare ice field is formed originally. As the origin of the bare ice, the redistribution of drifting snow is discussed in this section.

The redistribution of drifting snow can be seen in the distribution pattern of accumulation on the Antarctic Ice Sheet (GIOVINETTO and BULL, 1987). Along a stream line of katabatic wind, the accumulation gradually increases from the inland part (less than 50 mm/a) to the coast region (several hundred mm/a). However, in the middle part of the ice sheet, the accumulation decreases along the stream line, and shows almost zero and somewhere negative value; in the extreme case bare ice fields are formed such as the Yamato Bare Ice Field. TAKAHASHI (1988) calculated the redistribution of snow accumulation from the ice sheet topography and reduced the origin of Yamato Bare Ice Field to the surface erosion by this redistribution (TAKAHASHI *et al.*, 1989).

On the bare ice field at Seal Rock, the distribution of deposited snow is horseshoe-shaped. The same pattern of drifted snow is generally seen behind an obstacle in drifting snow. The bare ice field behind an obstacle can be explained by this redistribution of accumulation due to drifting snow.

If the ice sheet were thicker and Seal Rock were buried in the ice sheet in a previous age, the ice sheet surface would be smooth and covered with snow. When the ice sheet became thin for some reason and the top of the rock appeared, the drifting snow was diverted to both sides, and snow particles could not be supplied as the drifted snow just behind the rock. Under this condition, the surface is gradually eroded by sublimation, and a hard surface (particles are tightly bonded) appears.

Behind the rock as a obstacle, the wind speed once reduces, and gradually increases

along streamlines from the obstacle area, and also the transport ability of drifting snow gradually increases along the streamlines. As no snow particles entrain to air on the hard surface, the drifting snow is the "unsaturated" condition (the drift flux is smaller than the transport ability expected from wind speed). Under this condition, snow particles could not halt on the surface unless sufficient precipitation is supplied.

In this unsaturated condition, sublimation predominates on the surface, leaving bare ice from below the surface. Once the bare ice appears, the surface lowering is accelerated by sublimation due to the low albedo. If this surface lowering continues, the surface should lower infinitely. However, as a matter of fact, the lowering is not infinite and a stable surface topography is formed, which means that the mass loss of sublimation compensates the local ice flow due to topography.

On the Yamato Bare Ice Field, the origin of formation should be different from the case of Seal Rock, because there are no mountains windward of the ice field. Calculating the horizontal divergence of drift flux from the ice sheet topography, TAKAHASHI (1989) found that the positive divergence region coincided with the erosion area and the negative region with the accumulation area, and deduced that the origin is redistribution of drifting snow owing to the wind speed change caused by slope inclination change.

5. Classification of Ice Fields

The Seal Rock bare ice field is developed leeward of a bare rock which acts an obstacle to winds, whereas another type of bare ice field, Yamato bare ice field, is developed on a smooth surface of ice sheet without obstacles. Considering mechanism of formation, bare ice fields can be classified into four types. Typical bare ice fields are illustrated in Fig. 9. These types of bare ice field in the inland area of Antarctica are developed in the katabatic wind area where an enormous mass of drifting snow is transported in a year.

[A] *Obstacle origin group*

A1. *Obstacle-leeward type*

A bare ice field extends leeward from an obstacle, as seen in the Sør Rondane Mountains area. Leeward of Seal Rock, which rises about 100 m above the ice sheet surface, the length of the bare ice field is 4.5 km, while the length is about 15 km at Mt. Vesthausen with 300 m relative height and about 50 km at Mt. Romnoesfjellet with 500 m relative height. According to these relations, the length of bare ice fields is about 50 to 100 times the relative height of mountains.

A2. *Valley type*

In a mountain valley, bare ice is often seen on the glacier surface due to strong katabatic wind. As seen in the Sør Rondane Mountains area, the cold inland air mass flows down through a valley as a katabatic wind and eroded the surface, leaving bare ice.

[B] *No obstacle group (Ice-sheet topography group)*

B1. *Slope-change topography type (Two-dimensional topography type)*

On an ice sheet surface of convex topography, where surface slope increases along the wind direction, vast bare ice fields can extend, as on the Yamato bare ice

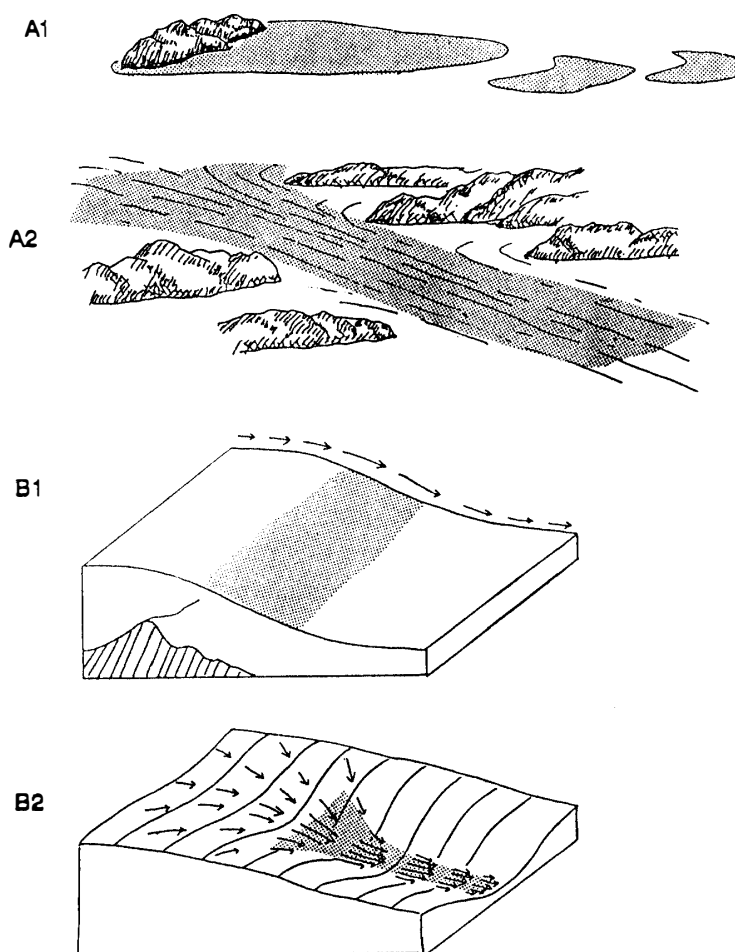


Fig. 9. Illustration of four types of bare ice fields. (Obstacle group) A1: Obstacle type, A2: Valley type. (No obstacle group) B1: Slope change type, B2: Basin type.

field. In this type of topography, the katabatic wind speed increases with increasing inclination and the drifting snow transport increases, eroding the surface and leaving bare ice (TAKAHASHI *et al.*, 1989).

B2. Basin topography type (Three-dimensional topography type)

In a large basin, katabatic winds converge to the bottom of the basin and wind speed increased by the funnel effect, which causes the formation of a bare ice field. On the Lambert Glacier drainage basin, MCINTYRE (1985) observed the distribution of bare ice fields from LANDSAT images, and found that they were developed in the strong katabatic wind area.

6. Concluding Remarks

Observations of meteorological components and ablation were carried out on the bare ice field leeward of Seal Rock in the Sør Rondane area, East Antarctica. Large sublimation (200 to 280 mm/a) was observed at bare ice field, and large accumulation (about 150 mm/a) was observed in the surrounding snow drift area. Air temperature on the bare ice was about 1°C higher than that on the snow surface.

Wind speeds on bare ice were about 1 m/s larger than on snow surface, which reflects the small roughness height on the bare ice surface.

The large sublimation on the bare ice can be explained from the low albedo of bare ice. Sublimation at Mizuho Station was well correlated with the solar radiation. Only from the relation between sublimation and solar radiation, the sublimation is estimated to be 670 mm/a as the maximum estimation. Taking the thermal properties of snow and ice into account, the estimation is corrected to 153 mm/a, which must be the minimum estimation. The observed values was ranged between these two estimations.

The origin of the bare ice field can be explained by the redistribution of drifting snow. The redistribution can be caused by obstacles or the change of wind speed due to the ice sheet topography.

Based on the origin of bare ice described above, the bare ice fields are roughly classified into 4 types: Obstacle-leeward type, Valley type, Slope-change topography type, and Basin topography type. The first two can be considered the "Obstacle origin group", and the last two the "No obstacle group".

Acknowledgments

The authors wish to express their sincere thanks to the members of the 30th Japanese Antarctic Research Expedition for their kind support in the observation of the bare ice field at Seal Rock.

References

- DE QUERVAIN, M. (1973): Snow structure, heat, and mass flux through snow. Role of Snow and Ice in Hydrology, Proceedings of the Banff Symposia, September 1972, Vol. 1, Paris, Unesco, 203-226 (IAHS Publ. No. 107).
- FUJII, Y. and KUSUNOKI, K. (1982): The role of sublimation and condensation in the formation of ice sheet surface at Mizuho Station, Antarctica. *J. Geophys. Res.*, **87**, 4293-4300.
- GIOVINETTO, M. B. and BULL, C. (1987): Summary and analyses of surface mass balance compilations for Antarctica, 1960-1985. *Byrd Polar Res. Center Rep.*, **1**, 90 p.
- GRENFELL, T. C. and PEROVICH, D. K. (1984): Spectral Albedos of sea ice and incident solar irradiance in the Southern Beaufort Sea. *J. Geophys. Res.*, **89**, 3573-3580.
- KOKURITSU KYOKUCHI KENKYŪJO (1985): Mizuho Kiti kikō-hyō (Mizuho Station climate table). *Nankyoku no Kagaku*, 9. Shiryō-hen (Science in Antarctica, 9. Data Compilation). Tokyo, Kokon Shoin, 78-80.
- MCINTYRE, N. F. (1985): A re-assessment of the mass balance of the Lambert Glacier drainage basin, Antarctica. *J. Glaciol.*, **31**, 34-38.
- NAGATA, T. (1978): A possible mechanism of concentration of meteorites within the Meteorite Ice Field in Antarctica. *Mem. Natl. Inst. Polar Res., Spec. Issue*, **8**, 70-92.
- OHATA, T., ISHIKAWA, N., KOBAYASHI, S. and KAWAGUCHI, S. (1985): Heat balance at the snow surface in a katabatic wind zone, East Antarctica. *Ann. Glaciol.*, **6**, 174-177.
- TAKAHASHI, S. (1988): A preliminary estimation of drifting snow convergence along a flow line of Shirase Glacier, East Antarctica. *Bull. Glacier Res.*, **6**, 41-46.
- TAKAHASHI, S., NARUSE, R. and MAE, S. (1989): A bare ice field in East Queen Maud Land, Antarctica, caused by horizontal divergence of drifting snow. *Ann. Glaciol.*, **11**, 156-160.
- YAMANOUCHI, T. (1983): Variation of incident solar flux and snow albedo on the solar zenith angle and cloud cover, at Mizuho Station, Antarctica. *J. Meteorol. Soc. Jpn.*, **61**, 879-893.

(Received March 23, 1991; Revised manuscript received October 25, 1991)